

# Synthesis and Structures of Hypervalent Antimony Compounds Bearing an Antimony–Group 6 Transition Metal Bond

Koichiro Toyota, Yohsuke Yamamoto, and Kin-ya Akiba\*

Department of Chemistry, Graduate School of Science, Hiroshima University,  
1-3-1 Kagamiyama, Higashi-Hiroshima 739-8526, Japan

Received September 12, 2000

Hypervalent pentacoordinate stiboranes with an Sb–group 6 element bond [ $\text{Rf}_2\text{Sb}^*\text{MCp}(\text{CO})_3$  { $\text{Rf} = o\text{-C}_6\text{H}_4\text{C}(\text{CF}_3)_2\text{O}$ -,  $\text{M} = \text{Cr}$  (**2**),  $\text{Mo}$  (**3**),  $\text{W}$  (**4**)}] were synthesized by the reaction of  $\text{Rf}_2\text{Sb}^*\text{-Li}^+$  (**1-Li**) with  $[\text{CpM}(\text{CO})_3]^+\text{BF}_4^-$ . X-ray crystallographic analysis of **2–4** showed that the geometry about the antimony atom is a distorted TBP structure with the  $\text{CpM}(\text{CO})_3$  fragment at the equatorial site of the TBP. Diastereomeric antimony compounds  $\text{RfRfm}^*\text{Sb}^*\text{MCp}(\text{CO})_3$  { $\text{Rfm}^* = o\text{-C}_6\text{H}_4\text{C}^*(\text{CF}_3)(\text{Me})\text{O}$ -,  $\text{M} = \text{Cr}$  (**10a,b**),  $\text{Mo}$  (**11a,b**),  $\text{W}$  (**12a,b**)} were synthesized by similar procedures. Each of the diastereomers could be separated by flash column chromatography, and the relative stereochemistry was determined by X-ray analysis. The pseudorotational barrier of **11a** at the central antimony atom was found to be very high (31.3 kcal/mol at 110 °C), showing the strong equatophilicity of the Mo fragment.

## Introduction

In the preceding paper<sup>1</sup> we reported the synthesis and isomerization of diastereomeric  $\text{RfRfm}^*\text{Sb}^*\text{FeCp}(\text{CO})_2$  (**15**) and  $\text{RfRfm}^*\text{Sb}^*\text{Fe}^*\text{Cp}(\text{CO})(\text{PPh}_3)$  (**15-PPh<sub>3</sub>**) and confirmed that isomerization of these complexes took place through a Berry pseudorotation process at the Sb atom. The energy barriers of the pseudorotation at the Sb atom in these compounds were determined to be high (30–33 kcal/mol); thus, the apicophilicity of the transition metal (group 8 element) fragments should be considered to be less than that of the *p*-tolyl group. However, the effects of group 6 elements on the properties of metalated hypervalent group 15 element compounds have not been made clear since most of the reported hypervalent group 15 element compounds with a group 6 element were unstable<sup>2</sup> or the hypervalent group 15 element (mostly phosphoranide) usually acted as a bidentate ligand coordinated to the molybdenum through the phosphorus and a heteroatom (N or O) in the ligands.<sup>3</sup> Although structural analysis of  $\text{Me}_2\text{Br}_2\text{-SbMCp}(\text{CO})_3$  ( $\text{M} = \text{Cr}, \text{Mo}, \text{W}$ ) was reported by Malish,<sup>4</sup> X-ray structural reports have been limited to compounds with a phosphorus–molybdenum bond<sup>2,3</sup> among group 6 transition metals. Here we report the preparation and X-ray analysis of stable hypervalent antimony compounds,  $\text{Rf}_2\text{Sb}^*\text{MCp}(\text{CO})_3$  { $\text{M} = \text{Cr}$  (**2**),  $\text{Mo}$  (**3**),  $\text{W}$  (**4**)}, bearing a series of group 6 transition metal ligands.<sup>5</sup>

To our knowledge, **2** is the first example of structurally characterized group 15 element compounds bearing a chromium fragment. In addition, diastereomeric hypervalent antimony compounds  $\text{RfRfm}^*\text{Sb}^*\text{MCp}(\text{CO})_3$  { $\text{Rfm}^* = o\text{-C}_6\text{H}_4\text{C}^*(\text{CF}_3)(\text{Me})\text{O}$ -,  $\text{M} = \text{Cr}$  (**10a,b**),  $\text{Mo}$  (**11a,b**),  $\text{W}$  (**12a,b**)} were synthesized, and the pseudorotational energy of **11a** was found to be slightly higher (31.3 kcal/mol at 110 °C) than that of the corresponding iron analogue (**15**; 30.5 kcal/mol at 110 °C). This result clearly indicated that the stereochemical rigidity of the stiboranes with an Sb–group 6 element (in this case Mo) bond was very high.

## Results and Discussion

**Preparation of  $\text{Rf}_2\text{Sb}^*\text{MCp}(\text{CO})_3$  { $\text{Rf} = o\text{-C}_6\text{H}_4\text{C}(\text{CF}_3)_2\text{O}$ -,  $\text{M} = \text{Cr}$  (**2**),  $\text{Mo}$  (**3**),  $\text{W}$  (**4**)}**. We have reported that  $\text{Rf}_2\text{Sb}^*\text{FeCp}(\text{CO})_2$ <sup>6</sup> was obtained in good yield (76%) by the reaction of stiboranide 10-Sb-4 anion,  $\text{Rf}_2\text{Sb}^*\text{-Et}_4\text{N}^+$ ,<sup>7</sup> with  $\text{CpFeI}(\text{CO})_2$ <sup>8</sup> in the presence of  $\text{AgBF}_4$ . Therefore, we tried to prepare hypervalent antimony compounds bearing a group 6 transition metal ligand by use of similar procedures. However, the reaction of stiboranide 10-Sb-4 anion  $\text{Rf}_2\text{Sb}^*\text{-Li}^+$  (**1-Li**) with  $\text{CpMoI}(\text{CO})_3$ <sup>9</sup> in the presence of  $\text{AgBF}_4$  gave only trace amounts (~3%) of  $\text{Rf}_2\text{Sb}^*\text{MoCp}(\text{CO})_3$  (**3**). Then, the reaction of  $\text{Rf}_2\text{Sb}^*\text{Cl}^{10}$  with  $[\text{CpMo}(\text{CO})_3]^- \text{Na}^+$ ,<sup>9</sup> generated from  $\text{Mo}(\text{CO})_6$  with  $\text{NaCp}$ , gave only a 10% yield of **3**. We found that the reaction of **1-Li** with  $[\text{CpMo}(\text{CO})_3]^+\text{BF}_4^-$ ,<sup>11</sup> generated by treatment of  $\text{CpMoH}(\text{CO})_3$ <sup>9</sup>

(1) Toyota, K.; Wakisaka, Y.; Yamamoto, Y.; Akiba, K.-y. *Organometallics* **2000**, *19*, 5122.

(2) Montgomery, C. D. *Phosphorus, Sulfur, Silicon* **1993**, *84*, 23 and references therein.

(3) (a) Khasnis, D. V.; Lattman, M.; Siriwardane, U. *Organometallics* **1991**, *10*, 1326. (b) Jeanneaux, F.; Grand, A.; Riess, J. G. *J. Am. Chem. Soc.* **1981**, *103*, 4272.

(4) Malisch, W.; Panster, P. H. *Angew. Chem., Int. Ed. Engl.* **1974**, *13*, 670.

(5) A part of this work has been previously communicated: Toyota, K.; Yamamoto, Y.; Akiba, K.-y. *Chem. Lett.* **1999**, 783.

(6) Yamamoto, Y.; Okazaki, M.; Wakisaka, Y.; Akiba, K.-y. *Organometallics* **1995**, *14*, 3364.

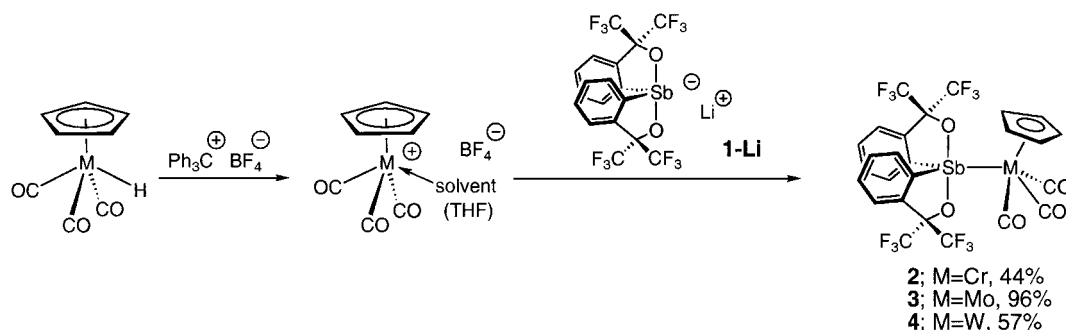
(7) Akiba, K.-y.; Nakata, H.; Yamamoto, Y.; Kojima, S. *Chem. Lett.* **1992**, 1559.

(8) King, R. B.; Stone, F. G. *Inorg. Synth.* **1963**, *7*, 110.

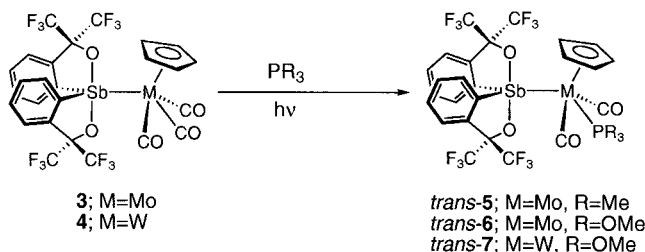
(9) Piper, T. S.; Wilkinson, G. J. *Inorg. Nucl. Chem.* **1956**, *3*, 104.

(10) Kojima, S.; Takagi, R.; Nakata, H.; Yamamoto, Y.; Akiba, K.-y. *Chem. Lett.* **1995**, 857.

Scheme 1



Scheme 2



with  $\text{Ph}_3\text{C}^+\text{BF}_4^-$ , gave a high yield (96%) of **3**, and chromium (**2**: 44%) and tungsten (**4**: 57%) adducts could be prepared by similar procedures (Scheme 1). These compounds were stable to atmospheric moisture, could be purified by column chromatography ( $\text{SiO}_2$ ,  $\text{CH}_2\text{Cl}_2$ : *n*-hexane = 1:1), and could be identified by NMR ( $^1\text{H}$  and  $^{19}\text{F}$ ), IR, elemental analysis, and X-ray structural analysis.

**Photoreaction of 3 and 4 with Trimethylphosphines or Trimethyl Phosphite.** The reaction of **3** with 1.5 equiv of  $\text{PMe}_3$  under irradiation with a tungsten lamp was monitored by  $^{19}\text{F}$  NMR spectrum. Some decomposition was observed, but it was found that *trans*- $\text{Rf}_2\text{Sb}^*\text{MoCp}(\text{CO})_2(\text{PMe}_3)$  (**5**) was obtained as the sole product. Similarly, the reaction of **3** or **4** with  $\text{P}(\text{OMe})_3$  also gave *trans*- $\text{Rf}_2\text{Sb}^*\text{MoCp}(\text{CO})_2(\text{P}(\text{OMe})_3)$  (**6**) or *trans*- $\text{Rf}_2\text{Sb}^*\text{WCp}(\text{CO})_2(\text{P}(\text{OMe})_3)$  (**7**), respectively (Scheme 2). In the reaction of **4** with  $\text{P}(\text{OMe})_3$ , the *cis*-isomer was observed in the early stage of the reaction, but the isomerization from *cis* to *trans* was too fast to isolate *cis*- $\text{Rf}_2\text{Sb}^*\text{W}^*\text{Cp}(\text{CO})_2(\text{P}(\text{OMe})_3)$ . These compounds, **5–7**, were stable to atmospheric moisture, could be purified by column chromatography ( $\text{SiO}_2$ , benzene: *n*-hexane = 1:1), and could be identified by NMR ( $^1\text{H}$ ,  $^{19}\text{F}$  and  $^{31}\text{P}$ ), elemental analysis, and X-ray structural analysis.

**Preparation of Diastereomeric  $\text{RfRfm}^*\text{Sb}^*\text{MCp}(\text{CO})_3$  { $\text{Rfm}^* = o\text{-C}_6\text{H}_4\text{C}^*(\text{CF}_3)(\text{Me})\text{O}^-$ , M = Cr (**10a,b**), Mo (**11a,b**), W (**12a,b**)}.  $\text{RfRfm}^*\text{Sb}^*\text{MCp}(\text{CO})_3$  {M = Cr (**10a,b**), Mo (**11a,b**), W (**12a,b**)}** were prepared by use of procedures similar to those of **2–4**, outlined in Scheme 3. Diastereomeric stiboranide anion  $\text{RfRfm}^*\text{Sb}^*-$   $\text{Et}_3\text{HN}^+$  (**9-Et<sub>3</sub>HN<sup>+</sup>**), generated from stibine  $\text{RfRfmH}^*\text{Sb}^*$  (**8**) and  $\text{NEt}_3$ , was used instead of **1-Li** to give complexes **10–12** in good yields. These complexes were stable to atmospheric moisture, and separation of diastereomers could be carried out by column chromatography ( $\text{SiO}_2$ ,  $\text{CH}_2\text{Cl}_2$ :*n*-hexane = 1:1). The relative stereochemistry

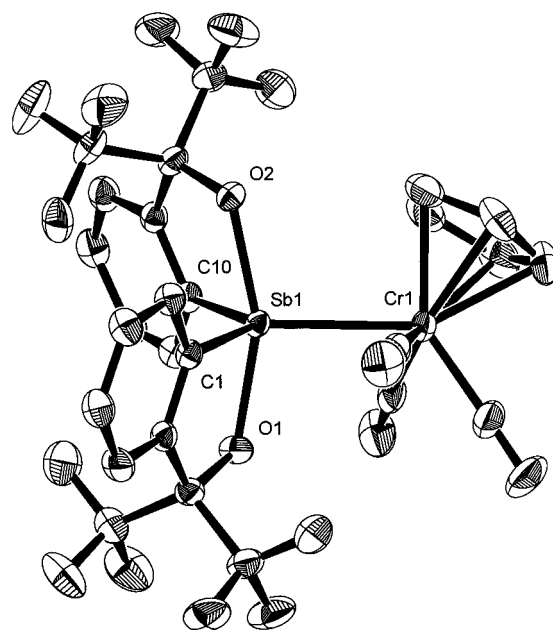


Figure 1. ORTEP diagram (30% probability ellipsoids) for **2**.

was assigned by X-ray structural analysis of **10b**, **11a**, and **12a** (vide infra). The ratio of diastereomers (**10a**:**10b** = 0.9:1, **11a**:**11b** = 1.5:1, **12a**:**12b** = 1.8:1) was different from that of **9-Et<sub>3</sub>HN<sup>+</sup>** (**9a**:**9b** = 9:1).<sup>10</sup> This fact indicated that diastereomer **b** of **9-Et<sub>3</sub>HN<sup>+</sup>** was more reactive toward bond formation than diastereomer **a** where equilibration between **a** and **b** of **9-Et<sub>3</sub>HN<sup>+</sup>** was taking place rapidly.

**X-ray Crystal Structures of 2, 3, and 4.** Crystals of **2** (Cr), **3** (Mo), and **4** (W) suitable for X-ray analysis were grown from  $\text{CH}_2\text{Cl}_2$ -*n*-hexane. Figures 1 and 2 show the ORTEP drawings of **2** and **3**. The structure of **4** (not cited) is almost completely identical to those of **2** and **3**. It is confirmed that the geometry about the antimony atom can be considered to be a distorted TBP structure with the  $\text{CpM}(\text{CO})_3$  fragment at the equatorial site of the TBP. Selected bond lengths and bond angles for **2**, **3**, and **4** are listed in Table 1. The average apical Sb–O lengths (2.089(2) Å in **2**, 2.093(3) Å in **3**, and 2.098(9) Å in **4**) are almost identical to that (2.087(3) Å) of  $\text{Rf}_2\text{Sb}^*\text{Fe}(\text{Cp})(\text{CO})_6$ <sup>6</sup> and that (2.083(2) Å) of  $\text{Rf}_2\text{Sb}^*\text{Ru}(\text{Cp})(\text{CO})_2$ <sup>1</sup> but are definitely longer than that of  $\text{Rf}_2\text{Sb}^*(p\text{-CH}_3\text{C}_6\text{H}_4)$  (2.039(3) Å).<sup>12</sup> In addition, the apical O–Sb–O angles (158.87(10)° in **2**, 163.8(1)° in **3**, 163.6-

(11) Markham, J.; Menard, K.; Culter, A. *Inorg. Chem.* **1985**, *24*, 1581.

(12) Kojima, S.; Doi, Y.; Okuda, M.; Akiba, K.-y. *Organometallics* **1995**, *14*, 1928.

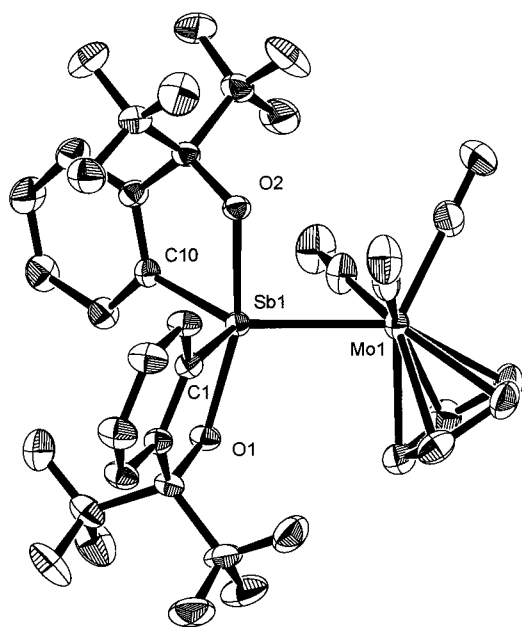
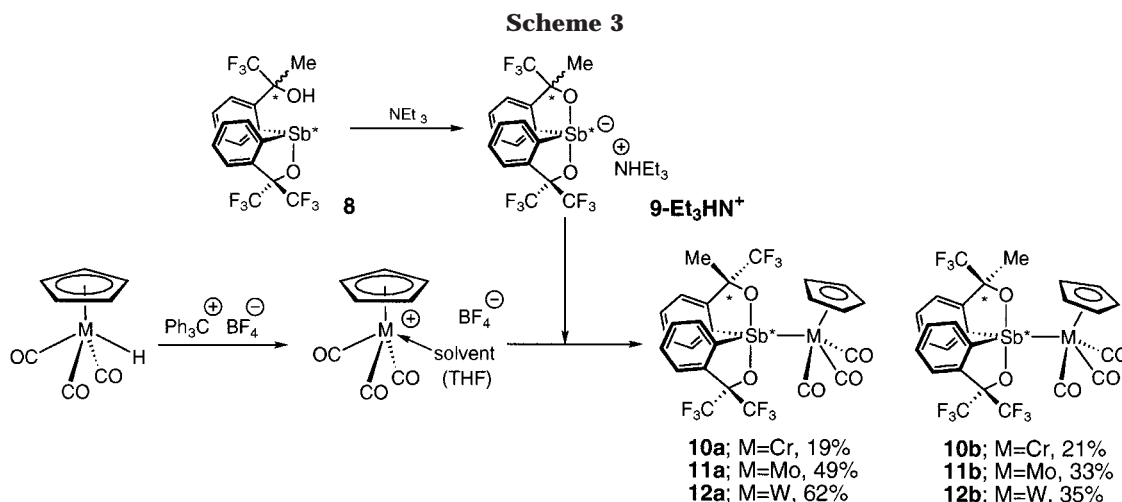


**Figure 2.** ORTEP diagram (30% probability ellipsoids) for **3**.

(4° in **4**) are comparable to that (162.5(1)°) of  $\text{Rf}_2\text{Sb}^*\text{Fe}(\text{Cp})(\text{CO})_2$  and that (161.1(1)°) of  $\text{Rf}_2\text{Sb}^*\text{Ru}(\text{Cp})(\text{CO})_2$  and are smaller than that (170.6(1)°) of  $\text{Rf}_2\text{Sb}^*(p\text{-CH}_3\text{C}_6\text{H}_4)$ . These facts are mainly due to the electron-donating property of the transition metal fragments  $\{\text{CpM}(\text{CO})_3$  (M = Cr, Mo, and W) and  $\text{CpM}(\text{CO})_2$  (M = Fe, and Ru) $\}$ , and the steric effect of the chromium fragment may play some role in narrowing the apical O–Sb–O angle of **2**. To our knowledge, **2** is the first example of structurally characterized group 15 element compounds bearing a chromium fragment.

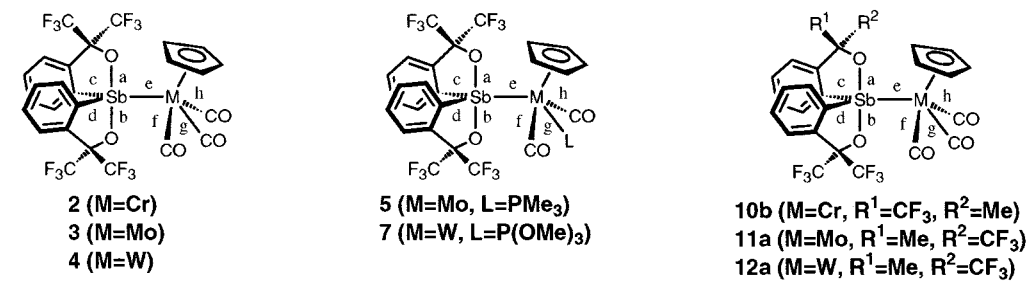
**X-ray Crystal Structures of 5 and 7.** Crystals of **5** and **7** suitable for X-ray analysis were grown from  $\text{CH}_2\text{Cl}_2$ –*n*-hexane. Figures 3 and 4 show the ORTEP drawings of **5** and **7**. Selected bond lengths and bond angles for **5** and **7** are listed in Table 1. When the bond lengths of the Sb–Mo bond (bond *e* in Table 1) of **3** and **5** (Mo) are compared, that (2.7380(4) Å) in **5** was shorter than that (2.761(3) Å) in **3**. The same trend was observed when the bond lengths of the Sb–W bond of **7** (2.732(2) Å) and **4** (2.765(2) Å) are compared. These facts are due to trans influence of the phosphine or phosphite ligand, and the increase in electron donation of the transition

metal ligands to the antimony atom is the reason for the shortening of the Sb–M bonds. In the corresponding iron compounds,  $\text{Rf}_2\text{Sb}^*\text{Fe}(\text{Cp})(\text{CO})_2$  (**15**) and  $\text{Rf}_2\text{Sb}^*\text{Fe}^*(\text{Cp})(\text{CO})(\text{PPh}_3)$  (**15-PPH<sub>3</sub>**),<sup>6</sup> this type of shortening of the Sb–Fe bond length was not observed; instead the Sb–Fe bond of **15-PPH<sub>3</sub>** (2.5204(5) and 2.5106(6) Å for each diastereomer) was even longer than that of **15** (2.4801(5) and 2.4790(5) Å for two independent molecules). Therefore, the origin of the donating property of the iron group can be ascribed to “ $\sigma$ -donation of the electropositive iron group into the central antimony atom” rather than to “donation from a filled d-orbital on Fe into the antibonding component of the axial MO on Sb in a  $\pi$ -fashion”, as was described in ref 6, note 21. Kubo et al., however, suggested  $\pi$ -back donation of an iron ligand in hypervalent phosphoranes.<sup>13</sup> Since the shortening of Sb–M bonds was observed due to the increase of the electron-donating property of group 6 metals, the donation from a filled d-orbital on group 6 metals into the antibonding component of the axial MO on Sb in a  $\pi$ -fashion should occur in this case. In consistent with the discussion, the averaged apical Sb–O bond length in **5** or **7** (2.112(2) Å in **5**, 2.11(1) Å in **7**) were slightly longer than those in **3** (2.093(3) Å) or **4** (2.098(9) Å), and the O–Sb–O angle in **5** or **7** (156.85(1)° in **5**, 157.3(5)° in **7**) was smaller than that in **3** (163.8(1)°) or **4** (163.6(4)°).

**X-ray Crystal Structures of 10b, 11a, and 12a.** Crystals of **10b** (Cr), **11a** (Mo), and **12a** (W) suitable for X-ray analysis were also obtained by recrystallization from  $\text{CH}_2\text{Cl}_2$ –*n*-hexane. Figures 5–7 show the ORTEP drawings of **10b**, **11a**, and **12a**. Thus, the relative stereochemistry of **10**–**12** was clearly determined. In these cases, it is also confirmed that the geometry about the antimony atom was similar to that of **2**–**4** and can be considered as a distorted TBP structure with the  $\text{CpM}(\text{CO})_3$  fragment at the equatorial site of the TBP. Selected bond lengths and bond angles for **10b**, **11a**, and **12a** are listed in Table 1. The averaged apical Sb–O lengths (2.075(4) Å in **10b**, 2.084(4) Å in **11a**, and 2.07(1) Å in **12a**) and the apical O–Sb–O angles (160.0(2)° in **10b**, 164.6(2)° in **11a**, 163.4(4)° in **12a**) are almost identical to those in **2**–**4**. The electron-donating property and the steric effect of the transition

(13) Kubo, K.; Nakazawa, H.; Miyoshi, K. *Organometallics* **1998**, *17*, 3522.

Table 1. Selected Bond Lengths and Bond Angles for 2, 3, 4, 5, 7, 10b, 11a, and 12a



	2	3	4	5	7	10b	11a	12a
Bond Lengths (Å)								
a	2.099(1)	2.099(3)	2.093(9)	2.088(2)	2.10(1)	2.072(4)	2.109(4)	2060(10)
b	2.079(3)	2.086(3)	2.102(8)	2.135(2)	2.12(1)	2.078(4)	2.059(4)	2.08(1)
c	2.117(2)	2.116(4)	2.09(1)	2.124(3)	2.12(3)	2.106(6)	2.112(7)	2.15(2)
d	2.101(3)	2.112(4)	2.10(1)	2.123(4)	2.12(2)	2.117(5)	2.112(7)	2.18(2)
e	2.6554(5)	2.761(3)	2.765(2)	2.7380(4)	2.732(2)	2.664(2)	2.764(3)	2.770(2)
f	1.861(5)	1.996(5)	1.99(2)	1.982(4)	2.01(2)	1.844(8)	1.990(10)	2.01(3)
g	1.884(4)	2.022(5)	1.97(2)	2.303(5)	2.36(4)	1.899(8)	2.023(8)	2.05(3)
h	1.876(4)	2.017(5)	2.00(1)	1.976(5)	1.97(2)	1.866(9)	2.026(9)	1.98(2)
Bond Angles (deg)								
ab	158.87(10)	163.8(1)	163.6(4)	156.85(10)	157.3(5)	160.0(2)	164.6(2)	163.4(4)
cd	117.2(1)	110.1(1)	109.0(5)	115.0(1)	119.0(8)	121.8(2)	109.7(3)	112.2(6)
ac	79.3(1)	79.1(1)	80.2(4)	78.8(1)	76.9(7)	80.2(2)	80.4(3)	78.1(6)
bd	79.2(1)	79.4(1)	78.7(4)	77.9(1)	80.0(7)	79.0(2)	78.7(2)	79.5(5)
ad	90.4(1)	90.6(1)	92.3(5)	88.3(1)	90.6(7)	90.8(2)	93.1(2)	89.2(5)
bc	89.1(1)	92.4(1)	89.8(4)	90.2(1)	89.6(6)	90.6(2)	90.1(2)	94.9(6)
ce	121.99(8)	124.2(1)	125.1(3)	122.20(10)	119.1(5)	117.5(2)	124.8(1)	123.5(4)
de	120.74(8)	125.5(1)	125.7(4)	122.82(10)	121.9(6)	120.6(2)	125.3(1)	124.0(5)
ae	102.42(6)	95.23(8)	100.7(3)	100.83(7)	100.8(4)	101.5(2)	100.1(1)	95.8(3)
be	98.70(8)	100.94(8)	95.7(3)	102.27(7)	101.7(3)	98.8(1)	95.2(1)	100.7(3)

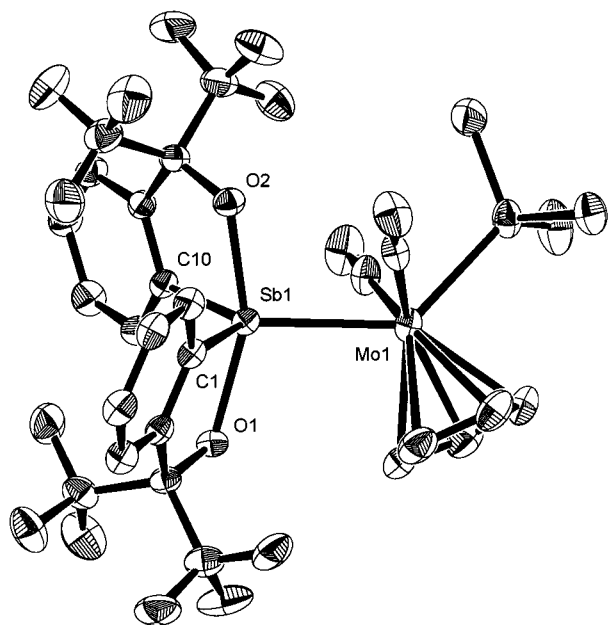


Figure 3. ORTEP diagram (30% probability ellipsoids) for 5.

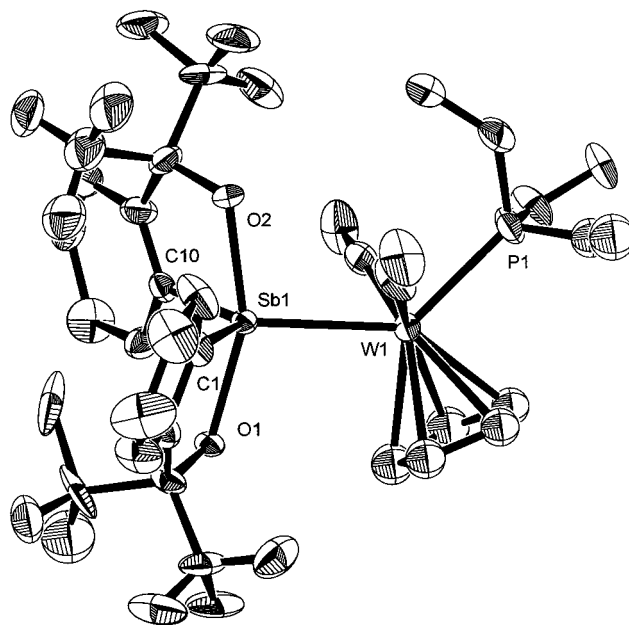
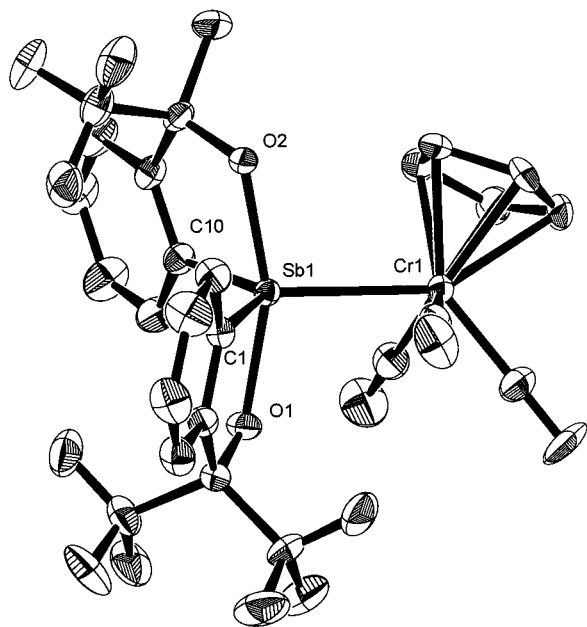


Figure 4. ORTEP diagram (30% probability ellipsoids) for 7.

metal fragments CpM(CO)<sub>3</sub> (M = Cr, Mo, and W) are also observed in these cases (Figures 5–7).

**Pseudorotational Barrier of 11a.** To investigate the pseudorotational barrier of hypervalent antimony compounds bearing a group 6 transition metal ligand, each diastereomer of **10** (Cr) (or **11** (Mo)) was dissolved in *o*-dichlorobenzene and was heated to monitor the isomerization by <sup>19</sup>F NMR. Unfortunately, we found that **10a** decomposed extensively up to 80 °C before isomerization took place. On the other hand, we could

observe the isomerization between **11a** and **11b** at 100, 110, 120, 130, and 140 °C to attain equilibrium (equilibrium ratio: **11a**:**11b** = 1:1.7 at 110 °C) without noticeable decomposition. Activation parameters for the isomerization of **11** are shown in Table 2 together with those of reference compounds. The small values of activation entropy ( $\Delta S^\ddagger$ ) [−2.7 (±5.9) (from **11a** to **11b**) and −0.9 (±4.8) eu (from **11b** to **11a**)] clearly suggest that the process should be intramolecular, that is, pseudorotation at the Sb atom. At 110 °C (383 K), the



**Figure 5.** ORTEP diagram (30% probability ellipsoids) for **10b**.

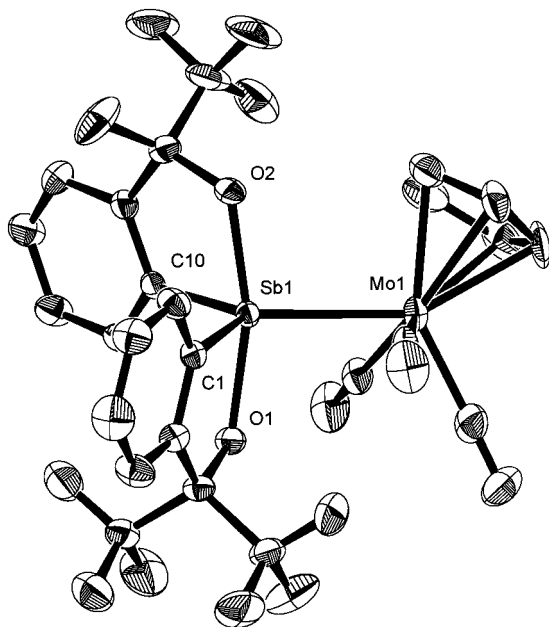


**Figure 6.** ORTEP diagram (30% probability ellipsoids) for **11a**.

pseudorotational barriers were 31.3 (**11a** to **11b**) and 31.7 kcal/mol (**11b** to **11a**), which were slightly higher than those of  $\text{RfRfm}^*\text{Sb}^*\text{FeCp}(\text{CO})_2$  (30.5 (**15a** to **15b**) and 30.2 kcal/mol (**15b** to **15a**)) and  $\text{RfRfm}^*\text{Sb}^*\text{RuCp}(\text{CO})_2$  (30.7 (**16a** to **16b**) and 30.4 kcal/mol (**16b** to **16a**))<sup>1</sup> and much higher than that of  $\text{Rf}_2\text{Sb}^*\text{Cl}$  (**13**; 14.6 kcal/mol)<sup>10</sup> and those of  $\text{RfRfm}^*\text{Sb}^*(p\text{-CH}_3\text{C}_6\text{H}_4)$  (28.1 kcal/mol (**14a** to **14b**), 27.7 kcal/mol (**14b** to **14a**))<sup>12</sup> (Table 2). Therefore, the strong "equatophilicity", which was observed in the iron and ruthenium compounds,<sup>1</sup> was confirmed in these cases, too. Although the energy difference between the group 6 (Mo) and the group 8 transition metals (Fe and Ru) was small, we might explain the difference on the basis of the electronic effect. In Allred-Rochow's electronegativity, molybdenum is the lowest among the three metals (Mo, 1.30;

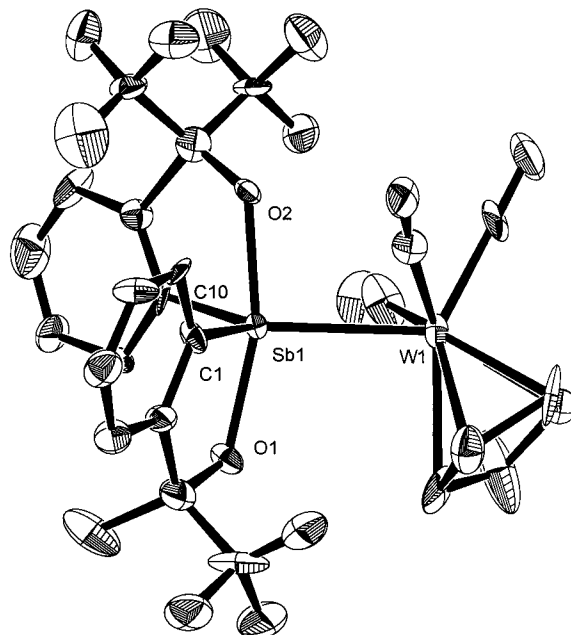


**Figure 7.** ORTEP diagram (30% probability ellipsoids) for **12a**.

Ru, 1.42; Fe, 1.64). In other words, the electron-donating effect of molybdenum is the highest; therefore, the  $\text{CpMo}(\text{CO})_3$  ligand would prefer the equatorial position strongly. In addition, on the basis of the discussion in our preceding paper,<sup>1</sup> steric effects of the phosphine ligand in  $\text{Rf}_2\text{Sb}^*\text{Fe}^*\text{Cp}(\text{CO})(\text{PR}_3)$  played some role in determining the pseudorotational barriers. Therefore, we think that the difference between (Fe and Ru) and Mo would be partly due to the steric bulkiness. The molybdenum ligand,  $\text{CpMo}(\text{CO})_3$ , has one extra CO ligand in comparison with the iron ligand,  $\text{CpFe}(\text{CO})_2$ , or the ruthenium ligand,  $\text{CpRu}(\text{CO})_2$ ; therefore, it can be regarded that the larger  $\text{CpMo}(\text{CO})_3$  ligand would prefer the equatorial position.

In conclusion, we prepared new pentacoordinate antimony compounds bearing a group 6 transition metal fragment and determined the pseudorotational barriers, which are much higher than those of the other carbon or halogen substituents. That is, the structures of the metalated hypervalent group 15 element compounds are stereochemically rigid. In considering the isolation of chiral five-coordinate phosphoranes,  $\text{Rf}_2\text{P}^*\text{R}$  (R = alkyl), by our group,<sup>14</sup> there is a possibility that the  $\text{Rf}_2\text{E}$  (E = group 15 main group element) ligand in some transition metal complexes can be useful as a new chiral ligand. Development of novel chiral catalysts bearing a hypervalent group 15 element-transition metal bond is currently under investigation.

## Experimental Section

Melting points were taken on a Yanagimoto micro melting point apparatus and are uncorrected. <sup>1</sup>H NMR (400-MHz), <sup>19</sup>F NMR (376-MHz), and <sup>31</sup>P NMR (162-MHz) spectra were recorded on a JEOL EX-400 spectrometer. Chemical shifts are reported ( $\delta$  scale) from internal  $\text{Me}_4\text{Si}$  for <sup>1</sup>H, from external  $\text{CFCl}_3$  for <sup>19</sup>F, or from external 85%  $\text{H}_3\text{PO}_4$  for <sup>31</sup>P. IR spectra

(14) Kojima, S.; Kajiyama, K.; Akiba, K.-y. *Bull. Chem. Soc. Jpn.* **1995**, *68*, 1785. Kojima, S.; Kajiyama, K.; Akiba, K.-y. *Tetrahedron Lett.* **1994**, *35*, 7037.

Table 2. Activation Parameters of 13, 14, 15, 16, and 11 for Berry Pseudorotation at the Sb Atom

	13 <sup>a</sup>	14 <sup>b</sup>	15 <sup>b</sup>	16 <sup>b</sup>	11 <sup>b</sup>
$\Delta G^\ddagger_{383K}(\text{kcal/mol})$					
a to b	14.6	28.1	30.5	30.7	31.3
b to a		27.7	30.2	30.4	31.7
$\Delta H^\ddagger(\text{kcal/mol})$					
a to b		28.5	29.6±0.6	28.3±0.2	30.3±2.4
b to a		28.2	29.0±0.6	27.9±0.1	31.4±2.3
$\Delta S^\ddagger(\text{eu})$					
a to b		1.06	-2.3±1.5	-6.2±0.4	-2.7±5.9
b to a		1.31	-3.1±1.5	-6.5±0.1	-0.9±4.8

a; toluene-*d*<sub>8</sub>, b; *o*-dichlorobenzene.

were recorded on a Shimadzu FTIR-8100A spectrometer. Elemental analysis was performed on a Perkin-Elmer 2400CHN elemental analyzer. Flash column chromatography was carried out on Merck silica gel 7734 or 9385. Thin-layer chromatography was performed with Merck silica gel 7730 or GF-254 plates. All reactions were carried out under dry Ar.

**Solvents and Reagents.** THF was freshly distilled from sodium-benzophenone, and CH<sub>2</sub>Cl<sub>2</sub>, 1,2-dichloroethane, and *o*-dichlorobenzene were freshly distilled from CaH<sub>2</sub> under dry N<sub>2</sub>. All other liquid reagents were also distilled from CaH<sub>2</sub> under dry N<sub>2</sub>. The preparation of CpMH(CO)<sub>3</sub> (M = Cr, Mo, W)<sup>9,15</sup> followed published procedures. The preparation of lithium stiboranide 10-Sb-4 anion (**1-Li**)<sup>6</sup> has been reported.

**Rf<sub>2</sub>Sb\*CrCp(CO)<sub>3</sub> (2).** In this case, CpCrH(CO)<sub>3</sub> was used without sublimation. Cr(CO)<sub>6</sub> (0.83 g, 3.77 mmol) was dissolved in 8 mL of THF, and NaCp (2.0 M in THF, 2.00 mL, 4.00 mmol) was added to the solution at room temperature. The mixture was heated under reflux for 18 h, followed by addition of 1 equiv of CH<sub>3</sub>COOH (0.22 mL, 3.77 mmol) at room temperature. The mixture was stirred for 15 min. All volatiles were removed in vacuo until the crude product containing CpCrH(CO)<sub>3</sub> was completely dried. The crude product was dissolved in 15 mL of CH<sub>2</sub>Cl<sub>2</sub>, and Ph<sub>3</sub>C<sup>+</sup>BF<sub>4</sub><sup>-</sup> (1.24 g, 3.77 mmol) was added to the solution to generate [CpCr(CO)<sub>3</sub>]<sup>+</sup>BF<sub>4</sub><sup>-</sup>. After 15 min of stirring at room temperature, **1-Li**<sup>+</sup> (0.77 g, 1.26 mmol) was added to the solution. The mixture was stirred for 3 h at room temperature and then filtered. After the solvent was removed in vacuo, Rf<sub>2</sub>Sb\*CrCp(CO)<sub>3</sub> (**2**) (0.45 g, 0.56 mmol) was obtained in 44% yield (based on Sb) in a pure form by column chromatography (SiO<sub>2</sub>, CH<sub>2</sub>Cl<sub>2</sub>:*n*-hexane = 1:1). Suitable crystals of **2** for X-ray structural analysis were obtained by recrystallization from CH<sub>2</sub>Cl<sub>2</sub>-*n*-hexane. **2**: yellow plates; mp 205–206 °C (dec); IR (KBr) 1955, 1970, 1977, 1986, 2000, 2035

cm<sup>-1</sup>; <sup>1</sup>H NMR (CDCl<sub>3</sub>) 5.18 (s, 5 H), 7.54 (t, 2 H, *J* = 7.8 Hz), 7.63 (t, 2 H, *J* = 7.8 Hz), 7.71 (d, 2 H, *J* = 7.8 Hz), 8.21 (d, 2 H, *J* = 7.8 Hz); <sup>19</sup>F NMR (CDCl<sub>3</sub>) -74.4 (q, 6 F, *J* = 9 Hz), -75.8 (q, 6 F, *J* = 9 Hz). Anal. Calcd for C<sub>26</sub>H<sub>13</sub>F<sub>12</sub>O<sub>5</sub>CrSb: C, 38.69; H, 1.62. Found: C, 39.04; H, 1.53.

**Rf<sub>2</sub>Sb\*MoCp(CO)<sub>3</sub> (3).** [CpMo(CO)<sub>3</sub>]<sup>+</sup>BF<sub>4</sub><sup>-</sup> was generated by treatment of freshly sublimed CpMoH(CO)<sub>3</sub> (1.19 g, 4.82 mmol) with Ph<sub>3</sub>C<sup>+</sup>BF<sub>4</sub><sup>-</sup> (1.59 g, 4.82 mmol) in 20 mL of dichloromethane at room temperature for 15 min, and **1-Li**<sup>+</sup> (1.50 g, 2.54 mmol) was added to the solution. The mixture was stirred for 3 h at room temperature and then filtered. After the solvent was removed in vacuo, Rf<sub>2</sub>Sb\*MoCp(CO)<sub>3</sub> (**3**) (2.00 g, 2.45 mmol) was obtained in 96% yield (based on Sb) in a pure form by column chromatography (SiO<sub>2</sub>, CH<sub>2</sub>Cl<sub>2</sub>:*n*-hexane = 1:1). Suitable crystals of **3** for X-ray structural analysis were obtained by recrystallization from CH<sub>2</sub>Cl<sub>2</sub>-hexane. **3**: yellow plates; mp 220–221 °C; IR (KBr) 1974, 1980, 1986, 2050 cm<sup>-1</sup>; <sup>1</sup>H NMR (CDCl<sub>3</sub>) 5.61 (s, 5 H), 7.52 (t, 2 H, *J* = 7.8 Hz), 7.61 (t, 2 H, *J* = 7.8 Hz), 7.70 (d, 2 H, *J* = 7.8 Hz), 8.17 (d, 2 H, *J* = 7.8 Hz); <sup>19</sup>F NMR (CDCl<sub>3</sub>) -74.4 (q, 6 F, *J* = 9 Hz), -75.8 (q, 6 F, *J* = 9 Hz). Anal. Calcd for C<sub>26</sub>H<sub>13</sub>F<sub>12</sub>O<sub>5</sub>MoSb: C, 36.69; H, 1.54. Found: C, 36.52; H, 1.41.

**Rf<sub>2</sub>Sb\*WCp(CO)<sub>3</sub> (4).** By use of procedures similar to those of **3**, Rf<sub>2</sub>Sb\*WCp(CO)<sub>3</sub> (**4**) (0.54 g, 0.57 mmol) was obtained in 57% yield (based on Sb) from CpWH(CO)<sub>3</sub> (0.52 g, 1.56 mmol), Ph<sub>3</sub>C<sup>+</sup>BF<sub>4</sub><sup>-</sup> (0.51 g, 1.56 mmol), and **1-Li**<sup>+</sup> (0.62 g, 1.01 mmol). **4**: yellow plates; mp 224–225 °C; IR (KBr) 1961, 1969, 1974, 2045 cm<sup>-1</sup>; <sup>1</sup>H NMR (CDCl<sub>3</sub>) 5.71 (s, 5 H), 7.52 (t, 2 H, *J* = 7.8 Hz), 7.61 (t, 2 H, *J* = 7.8 Hz), 7.70 (d, 2 H, *J* = 7.8 Hz), 8.15 (d, 2 H, *J* = 7.8 Hz); <sup>19</sup>F NMR (CDCl<sub>3</sub>) -74.3 (q, 6 F, *J* = 9 Hz), -75.8 (q, 6 F, *J* = 9 Hz). Anal. Calcd for C<sub>26</sub>H<sub>13</sub>F<sub>12</sub>O<sub>5</sub>WSb: C, 33.26; H, 1.40. Found: C, 33.25; H, 1.30.

**trans-Rf<sub>2</sub>Sb\*MoCp(CO)<sub>2</sub>(PMe<sub>3</sub>) (5).** A solution of **3** (70.4 mg, 0.083 mmol) and trimethylphosphine (13 μL, 0.126 mmol) in 2 mL of 1,2-dichloroethane was irradiated with a tungsten

Table 3. Crystal Data for 2, 3, 4, 5, 7, 10b, 11a, and 12a

	2	3	4	5	7	10b	11a	12a
formula	C <sub>26</sub> H <sub>13</sub> O <sub>5</sub> F <sub>12</sub> CrSb	C <sub>26</sub> H <sub>13</sub> O <sub>5</sub> F <sub>12</sub> MoSb	C <sub>26</sub> H <sub>13</sub> O <sub>5</sub> F <sub>12</sub> SbW	C <sub>28</sub> H <sub>22</sub> O <sub>4</sub> F <sub>12</sub> MoPSb	C <sub>28</sub> H <sub>22</sub> O <sub>7</sub> F <sub>12</sub> PSbW	C <sub>26</sub> H <sub>16</sub> O <sub>5</sub> F <sub>9</sub> CrSb	C <sub>26</sub> H <sub>16</sub> O <sub>5</sub> F <sub>9</sub> MoSb	C <sub>26</sub> H <sub>16</sub> O <sub>5</sub> F <sub>9</sub> SbW
mol wt	807.10	851.10	938.98	899.10	1035.04	753.10	797.10	885.01
cryst syst	monoclinic	monoclinic	monoclinic	monoclinic	orthorhombic	orthorhombic	monoclinic	monoclinic
space group	P2 <sub>1</sub> /c	P2 <sub>1</sub> /n	P2 <sub>1</sub> /n	P2 <sub>1</sub> /n	Iba2	Aba2	P2 <sub>1</sub> /n	P2 <sub>1</sub> /n
cryst dimens, mm	0.75 × 0.60 × 0.40	0.35 × 0.30 × 0.12	0.80 × 0.50 × 0.35	0.45 × 0.30 × 0.20	0.95 × 0.70 × 0.30	0.90 × 0.50 × 0.25	0.70 × 0.50 × 0.25	0.48 × 0.30 × 0.20
a, Å	15.596(6)	9.78(1)	9.799(6)	15.524(5)	15.639(9)	18.77(1)	9.681(8)	9.706(5)
b, Å	11.881(4)	34.29(4)	34.16(2)	18.109(6)	38.23(2)	18.661(8)	34.14(2)	34.07(1)
c, Å	15.184(5)	9.08(1)	9.090(5)	12.296(4)	11.661(8)	15.395(7)	9.029(5)	9.013(4)
α, deg	90	90	90	90	90	90	90	90
β, deg	101.28(3)	114.14(9)	114.30(4)	111.95(3)	90	90	114.28(5)	114.33(4)
γ, deg	90	90	90	90	90	90	90	90
V, Å <sup>3</sup>	2759.4(1)	2779.8(1)	2773.2(1)	3206.0(1)	6971.0(1)	5393.9(1)	2720.4(1)	2715.8(1)
Z	4	4	4	4	8	8	4	4
D <sub>calc</sub> , g cm <sup>-3</sup>	1.942	2.033	2.249	1.862	1.972	1.855	1.946	2.164
abs coeff, cm <sup>-1</sup>	1.4843	1.5325	1.3788	1.3788	4.2972	1.4966	1.5441	5.4207
F(000)	1568	1640	1768	1752	3952	2944	1544	1672
radiation,	Mo Kα; 0.710 73	Mo Kα; 0.710 73	Mo Kα; 0.710 73	Mo Kα; 0.710 73	Mo Kα; 0.710 73	Mo Kα; 0.710 73	Mo Kα; 0.710 73	Mo Kα; 0.710 73
λ, Å	298	298	298	298	298	298	298	298
temp, K	55	55	55	55	55	55	55	60
2θ max, deg	4.0	4.0	4.0	4.0	4.0	4.0	4.0	4.0
scan rate, deg/min	5.2	5.8	3.8	13.5	4.7	3.4	2.9	13.0
linear decay, %	+h, +k, ±l	±h, -k, +l	±h, +k, +l	+h, -k, ±l	-h, +k, +l	-h, +k, +l	+h, -k, ±l	+h, -k, ±l
data collcd	6648, 6349,	6883, 6426,	6836, 6378,	4527, 4296,	5214, 5160,	4114, 4069,	6658, 6239,	6741, 6317,
tot. data collcd,	5770 (I > 3σ(I))	5255 (I > 3σ(I))	4801 (I > 3σ(I))	3767 (I > 3σ(I))	4540 (I > 3σ(I))	3428 (I > 3σ(I))	5291 (I > 3σ(I))	5527 (I > 3σ(I))
unique, obsd	0.058	0.026	0.028	0.019	0.018	0.023	0.026	0.073
R int	406	406	406	424	411	379	379	379
no. of params refined	0.039, 0.074,	0.040, 0.058,	0.064, 0.124,	0.027, 0.058,	0.102, 0.133,	0.046, 0.063,	0.051, 0.117, 1.661	0.116, 0.225, 2.220
R, R <sub>w</sub> , GOF	1.267	1.093	1.185	1.133	1.313	0.826	0.1020	0.0070
max shift in final cycle	0.0100	0.0010	0.0010	0.0020	0.3113	0.0150	0.1020	0.0070
final cycle	1.03	1.33	2.78	0.76	7.94	0.97	1.34	4.85
max, e/Å <sup>3</sup>								

lamp for 8 h at room temperature. After the solvent was removed in vacuo, the crude products were subjected to flash column chromatography (SiO<sub>2</sub>, benzene:*n*-hexane = 1:1) to obtain pure **5** (22.4 mg, 0.025 mmol) in 30% yield. Suitable crystals of **5** for X-ray structural analysis were obtained by recrystallization from CH<sub>2</sub>Cl<sub>2</sub>-*n*-hexane. **5**: yellow plates; mp 296–298 °C (dec); <sup>1</sup>H NMR (CDCl<sub>3</sub>) 1.62 (d, 9 H, <sup>2</sup>J<sub>P-H</sub> = 9.8 Hz), 5.23 (d, 5 H, <sup>3</sup>J<sub>P-H</sub> = 1.4 Hz), 7.45 (t, 2 H, *J* = 7.3 Hz), 7.56 (t, 2 H, *J* = 7.3 Hz), 7.64 (d, 2 H, *J* = 7.3 Hz), 8.22 (d, 2 H, *J* = 7.3 Hz); <sup>19</sup>F NMR (CDCl<sub>3</sub>) -74.1 (q, 6 F, *J* = 9 Hz), -75.7 (q, 6 F, *J* = 9 Hz); <sup>31</sup>P NMR (CDCl<sub>3</sub>) 23.1 (s, 1 P). Anal. Calcd for C<sub>28</sub>H<sub>22</sub>F<sub>12</sub>O<sub>4</sub>MoPSb: C, 37.40; H, 2.47. Found: C, 37.31; H, 2.21.

**trans-Rf<sub>2</sub>Sb\*MoCp(CO)<sub>2</sub>(P(OMe)<sub>3</sub>) (6)**. By use of procedures similar to those of **5**, *trans*-Rf<sub>2</sub>Sb\*MoCp(CO)<sub>2</sub>(P(OMe)<sub>3</sub>) (**6**) (58.0 mg, 0.061 mmol) was obtained in 90% yield from **3** (58.2 mg, 0.068 mmol) and trimethyl phosphite (10 μL, 0.085 mmol). **6**: yellow plates; mp 247–248 °C (dec); <sup>1</sup>H NMR (CDCl<sub>3</sub>) 3.68 (d, 9 H, <sup>3</sup>J<sub>P-H</sub> = 11.7 Hz), 5.37 (s, 5 H), 7.46 (t, 2 H, *J* = 7.8 Hz), 7.56 (t, 2 H, *J* = 7.8 Hz), 7.64 (d, 2 H, *J* = 7.8 Hz), 8.19 (d, 2 H, *J* = 7.8 Hz); <sup>19</sup>F NMR (CDCl<sub>3</sub>) -73.5 (q, 6 F, *J* = 9 Hz), -75.6 (q, 6 F, *J* = 9 Hz); <sup>31</sup>P NMR (CDCl<sub>3</sub>) 182.4 (s, 1 P). Anal. Calcd for C<sub>28</sub>H<sub>22</sub>F<sub>12</sub>O<sub>7</sub>MoPSb + 0.5 CH<sub>2</sub>Cl<sub>2</sub>: C, 34.59; H, 2.34. Found: C, 34.97; H, 2.24.

**trans-Rf<sub>2</sub>Sb\*WCp(CO)<sub>2</sub>(P(OMe)<sub>3</sub>) (7)**. By use of procedures similar to those of **5**, *trans*-Rf<sub>2</sub>Sb\*WCp(CO)<sub>2</sub>(P(OMe)<sub>3</sub>) (**7**) (43.8 mg, 0.042 mmol) was obtained in 92% yield from **4** (43.6 mg, 0.046 mmol) and trimethyl phosphite (6.6 μL, 0.056 mmol). Suitable crystals of **7** for X-ray structural analysis were obtained by recrystallization from CH<sub>2</sub>Cl<sub>2</sub>-hexane. **7**: yellow plates; mp 247–248 °C; <sup>1</sup>H NMR (CDCl<sub>3</sub>) 3.68 (d, 9 H, <sup>3</sup>J<sub>P-H</sub> = 13.7 Hz), 5.45 (d, 5 H, <sup>3</sup>J<sub>P-H</sub> = 2.4 Hz), 7.45 (t, 2 H, *J* = 7.3 Hz), 7.56 (t, 2 H, *J* = 7.3 Hz), 7.62 (d, 2 H, *J* = 7.3 Hz), 8.16 (d, 2 H, *J* = 7.3 Hz); <sup>19</sup>F NMR (CDCl<sub>3</sub>) -73.8 (q, 6 F, *J* = 10 Hz), -75.7 (q, 6 F, *J* = 10 Hz); <sup>31</sup>P NMR (CDCl<sub>3</sub>) 144.2 (d, 1 P, <sup>1</sup>J<sub>P-W</sub> = 199 Hz). Anal. Calcd for C<sub>28</sub>H<sub>22</sub>F<sub>12</sub>O<sub>7</sub>PSbW + CH<sub>2</sub>Cl<sub>2</sub>: C, 31.10; H, 2.16. Found: C, 30.73; H, 2.11.

**RfRfm\*Sb\*CrCp(CO)<sub>3</sub> (10a and 10b)**. A suspension of [CpCr(CO)<sub>3</sub>]<sup>+</sup>BF<sub>4</sub><sup>-</sup> was generated from the reaction of CpCrH(CO)<sub>3</sub> [Cr(CO)<sub>6</sub>, 240 mg, 1.1 mmol; NaCp (2.0 M in THF), 0.65 mL, 1.3 mmol; CH<sub>3</sub>COOH, 63 μL, 1.1 mmol; THF, 5 mL] and Ph<sub>3</sub>C<sup>+</sup>BF<sub>4</sub><sup>-</sup> (363 mg, 1.1 mmol) in 10 mL of THF at room temperature for 15 min. To the suspension was added **9-Et<sub>3</sub>HN<sup>+</sup>** generated from RfRfmH\*Sb\* (**8**) (200 mg, 0.36 mmol) and NEt<sub>3</sub> (51 μL, 0.37 mmol) in 10 mL of THF at room temperature. The mixture was stirred for 1 h at room temperature. After the solvent was removed in vacuo, the crude products were subjected to flash column chromatography (SiO<sub>2</sub>, CH<sub>2</sub>Cl<sub>2</sub>:*n*-hexane = 1:1) to separate the diastereomers (**10a** and **10b**). Suitable crystals of **10b** for X-ray structural analysis were obtained by recrystallization from CH<sub>2</sub>Cl<sub>2</sub>-*n*-hexane. **10a**: 51 mg, 0.067 mmol, 19% (based on Sb), yellow plates; mp 204–205 °C (dec); IR (KBr) 1966, 1973, 2031 cm<sup>-1</sup>; <sup>1</sup>H NMR (CDCl<sub>3</sub>) 1.52 (s, 3 H), 5.12 (s, 5 H), 7.0–8.3 (m, 8 H); <sup>19</sup>F NMR (CDCl<sub>3</sub>) -74.9 (q, 3 F, *J* = 9 Hz), -75.4 (q, 3 F, *J* = 9 Hz), -78.3 (s, 3 F). Anal. Calcd for C<sub>26</sub>H<sub>16</sub>F<sub>9</sub>O<sub>5</sub>CrSb: C, 41.46; H, 2.14. Found: C, 41.31; H, 2.41. **10b**: 56 mg, 0.075 mmol, 21% (based on Sb), yellow plates; mp 195–198 °C (dec); IR (KBr) 1968, 1977, 2030 cm<sup>-1</sup>; <sup>1</sup>H NMR (CDCl<sub>3</sub>) 1.61 (s, 3 H), 5.13 (s, 5 H), 7.0–8.1 (m, 8 H); <sup>19</sup>F NMR (CDCl<sub>3</sub>) -74.7 (q, 3 F, *J* = 9 Hz), -76.1 (q, 3 F, *J* = 9 Hz), -79.9 (s, 3 F). Anal. Calcd for C<sub>26</sub>H<sub>16</sub>F<sub>9</sub>O<sub>5</sub>CrSb: C, 41.46; H, 2.14. Found: C, 41.62; H, 2.14.

**RfRfm\*Sb\*MoCp(CO)<sub>3</sub> (11a and 11b)**. By use of procedures similar to those of **10a** and **10b**, the diastereomers (**11a** and **11b**) were obtained from CpMoH(CO)<sub>3</sub> [Mo(CO)<sub>6</sub>, 290 mg, 1.1 mmol; NaCp (2.0 M in THF), 0.65 mL, 1.3 mmol; CH<sub>3</sub>COOH, 63 μL, 1.1 mmol; THF, 5 mL], Ph<sub>3</sub>C<sup>+</sup>BF<sub>4</sub><sup>-</sup> (363 mg, 1.1 mmol), and **9-Et<sub>3</sub>HN<sup>+</sup>** (**8**, 200 mg, 0.36 mmol; NEt<sub>3</sub>, 51 μL, 0.37 mmol). Suitable crystals of **11a** for X-ray structural analysis were obtained by recrystallization from CH<sub>2</sub>Cl<sub>2</sub>-*n*-

hexane. **11a**: 140 mg, 0.18 mmol, 49% (based on Sb); yellow plates; mp 204–205 °C (dec); IR (KBr) 1966, 1973, 2031 cm<sup>-1</sup>; <sup>1</sup>H NMR (CDCl<sub>3</sub>) 1.49 (s, 3 H), 5.63 (s, 5 H), 7.42–7.51 (m, 4 H), 7.57 (t, 1 H, *J* = 7.3 Hz), 7.69 (d, 1 H, *J* = 7.3 Hz), 8.11 (d, 1 H, *J* = 7.3 Hz), 8.21 (d, 1 H, *J* = 7.3 Hz); <sup>19</sup>F NMR (CDCl<sub>3</sub>) -74.8 (q, 3 F, *J* = 10 Hz), -75.4 (q, 3 F, *J* = 10 Hz), -78.4 (s, 3 F). Anal. Calcd for C<sub>26</sub>H<sub>16</sub>F<sub>9</sub>O<sub>5</sub>MoSb: C, 39.18; H, 2.03. Found: C, 38.96; H, 2.03. **11b**: 95 mg, 0.12 mmol, 33% (based on Sb), yellow plates; mp 195–198 °C (dec); IR (KBr) 1968, 1977, 2030 cm<sup>-1</sup>; <sup>1</sup>H NMR (CDCl<sub>3</sub>) 1.72 (s, 3 H), 5.62 (s, 5 H), 7.45–7.61 (m, 5 H), 7.71 (d, 1 H, *J* = 7.3 Hz), 8.10 (d, 1 H, *J* = 7.3 Hz), 8.14 (d, 1 H, *J* = 7.3 Hz); <sup>19</sup>F NMR (CDCl<sub>3</sub>) -74.8 (q, 3 F, *J* = 9 Hz), -76.2 (q, 3 F, *J* = 9 Hz), -79.9 (s, 3 F). Anal. Calcd for C<sub>26</sub>H<sub>16</sub>F<sub>9</sub>O<sub>5</sub>MoSb: C, 39.18; H, 2.03. Found: C, 39.15; H, 2.13.

**RfRfm\*Sb\*WCp(CO)<sub>3</sub> (12a and 12b)**. By use of procedures similar to those of **10a** and **10b**, the diastereomers (**12a** and **12b**) were obtained from CpWH(CO)<sub>3</sub> [W(CO)<sub>6</sub>, 387 mg, 1.1 mmol; NaCp (2.0 M in THF), 0.75 mL, 1.5 mmol; CH<sub>3</sub>COOH, 63 μL, 1.1 mmol; THF, 5 mL], Ph<sub>3</sub>C<sup>+</sup>BF<sub>4</sub><sup>-</sup> (363 mg, 1.1 mmol), and **9-Et<sub>3</sub>HN<sup>+</sup>** (**8**, 202 mg, 0.37 mmol; NEt<sub>3</sub>, 51 μL, 0.37 mmol). Suitable crystals of **12a** for X-ray structural analysis were obtained by recrystallization from CH<sub>2</sub>Cl<sub>2</sub>-*n*-hexane. **12a**: 201 mg, 0.23 mmol, 62% (based on Sb), yellow plates; mp 213–214 °C (dec); <sup>1</sup>H NMR (CDCl<sub>3</sub>) 1.48 (s, 3 H), 5.73 (s, 5 H), 7.44–7.59 (m, 5 H), 7.69 (d, 1 H, *J* = 7.3 Hz), 8.09 (d, 1 H, *J* = 7.3 Hz), 8.19 (d, 1 H, *J* = 7.3 Hz); <sup>19</sup>F NMR (CDCl<sub>3</sub>) -74.7 (q, 3 F, *J* = 10 Hz), -75.4 (q, 3 F, *J* = 10 Hz), -78.3 (s, 3 F). Anal. Calcd for C<sub>26</sub>H<sub>16</sub>F<sub>9</sub>O<sub>5</sub>WSb: C, 35.29; H, 1.82. Found: C, 35.55; H, 1.74. **12b**: 116 mg, 0.13 mmol, 33% (based on Sb), yellow plates; mp 195–198 °C (dec); <sup>1</sup>H NMR (CDCl<sub>3</sub>) 1.71 (s, 3 H), 5.70 (s, 5 H), 7.44–7.60 (m, 5 H), 7.70 (d, 1 H, *J* = 7.3 Hz), 8.06 (d, 1 H, *J* = 7.3 Hz), 8.11 (d, 1 H, *J* = 7.3 Hz); <sup>19</sup>F NMR (CDCl<sub>3</sub>) -74.8 (q, 3 F, *J* = 10 Hz), -76.2 (q, 3 F, *J* = 10 Hz), -80.0 (s, 3 F). Anal. Calcd for C<sub>26</sub>H<sub>16</sub>F<sub>9</sub>O<sub>5</sub>WSb: C, 35.29; H, 1.82. Found: C, 35.46; H, 1.88.

**Measurement of Positional Isomerization of 11a to 11b**. A solution of **11a** (ca. 10 mg) in 0.6 mL of dry *o*-dichlorobenzene was sealed in an NMR tube under dry N<sub>2</sub> for each kinetic run. The temperatures for the kinetic runs were maintained at 100 (± 1), 110 (± 1), 120 (± 1), 130 (± 1), and 140 (± 1) °C in an NMR probe. The composition of the diastereomers was monitored by integration of <sup>19</sup>F NMR signals. The data were analyzed by assuming first-order kinetics.

**Crystal Structure of 2, 3, 4, 5, 7, 10b, 11a, and 12a**. Crystal data and numerical details of the structural determinations are given in Table 3. Crystals were mounted on a Mac Science MXC3 diffractometer and irradiated with graphite-monochromated Mo Kα radiation (λ = 0.71073 Å) for data collection. Lattice parameters were determined by least-squares fitting of 29 reflections with 24° < 2θ < 28° in **2**, of 29 reflections with 26° < 2θ < 30° in **3**, of 31 reflections with 21° < 2θ < 25° in **4**, of 31 reflections with 31° < 2θ < 35° in **5**, of 31 reflections with 26° < 2θ < 30° in **7**, of 31 reflections with 31° < 2θ < 35° in **10b**, of 31 reflections with 26° < 2θ < 29° in **11a**, and of 29 reflections with 31° < 2θ < 35° in **12a**. Data were collected with the 2θ/ω scan mode. All data were corrected for absorption based on ψ scan<sup>16</sup> and extinction.<sup>17</sup> The structures were solved by a direct method with the program Crystan-GM (Mac Science)<sup>18</sup> and by refined full-matrix least squares. All non-hydrogen atoms were refined with anisotropic thermal parameters. All hydrogen atoms could be found on a difference Fourier map; these coordinates were included in the refinement with isotropic thermal parameters.

(16) Furusaki, A. *Acta Crystallogr.* **1979**, *A35*, 220.

(17) Katayama, C. *Acta Crystallogr.* **1986**, *A42*, 19.

(18) The program is available from MacScience Co.



**Acknowledgment.** We thank to Central Glass Co. for supplying us with 1,1-bis(trifluoromethyl)benzyl alcohol. Part of this work was supported by Grants-in-Aid for Scientific Research (Nos. 09239103, 09440218, 11166248, 11304044) from the Ministry of Education, Science, Sports, and Culture, Japan.

**Supporting Information Available:** Positional and thermal parameters and interatomic distances and angles for **2**, **3**, **4**, **5**, **7**, **10b**, **11a**, and **12a**. This material is available free of charge via the Internet at <http://pubs.acs.org>.

OM000791D